In memory of T. A. Stephenson

The Syntheses and Crystal and Molecular Structures * of some Ten-vertex (MCB_8; M = Ru or Os) Metallacarbaboranes: 9,9,9-(CO)$(PPh_3)_2$-*nido*-9,6-MCB_8H_{10}-5-(PPh_3)] (M = Ru or Os) and [9,9,9-(η-C_5H_5)(H)(PPh_3)-*arachno*-9,6-$RuCB_8H_{12}$]

Nathaniel W. Alcock, Michael J. Jasztal, and Malcolm G. H. Wallbridge
Department of Chemistry, University of Warwick, Coventry CV4 7AL

The reaction of [MCl(CO)(H)$(PPh_3)_3$] (M = Ru or Os) with *arachno*-$[CB_8H_{13}]^-$ yields the *nido*-metallacarbaboranes [9,9,9-(CO)$(PPh_3)_2$-9,6-MCB_8H_{10}-5-(PPh_3)] [M = Ru (**1**) or Os (**2**)] in reasonable yields as red and orange crystals respectively. A phosphine ligand is transferred from the metal atom to the cage in each case, and they both show a decaborane(14)-like cage structure with the 6- and 9-positions occupied by CH and M(CO)$(PPh_3)_2$ fragments respectively, as confirmed by single-crystal *X*-ray diffraction analysis. Compounds (**1**) and (**2**) are isostructural and isomorphous with their crystals monoclinic, space group $P2_1/n$, with $Z = 4$. $R = 0.087$ for 2 670 observed [$I/\sigma(I) \geqslant 3.0$] reflections for (**1**) and 0.050 for 3 525 observed reflections for (**2**) respectively. A similar reaction with [RuCl(η-C_5H_5)$(PPh_3)_2$] yields the *arachno* species [9,9,9-(η-C_5H_5)(H)(PPh_3)-9,6-$RuCB_8H_{12}$], (**3**). In this case the cage arrangement as determined by a single-crystal *X*-ray diffraction study, is similar to that in $[B_{10}H_{14}]^{2-}$ with the 6-and 9-positions substituted by CH_2 and RuH(η-C_5H_5)(PPh_3) fragments respectively. The crystals are monoclinic, space group $P2_1/n$, with $Z = 4$, $R = 0.046$ for 3 523 observed reflections. The application of the skeletal electron counting rules to this *arachno* structure is discussed.

A variety of ten-vertex polyhedra containing metal and boron atoms in the framework (*e.g.*, MB_9) are known.[1] Many of these adopt a *nido* structure,[2] based on *nido*-decaborane(14), but *closo*[3] and bimetallic (M_2B_8) *nido* frameworks[4] have also been identified. By comparison the range of ten-vertex systems containing a further heteroatom, as in the metallacarbaboranes based on MCB_8, is limited, and further examples are required before bonding and structural trends become apparent. To date such compounds have been prepared containing metals in the cobalt and nickel groups, and include *nido* compounds containing iridium[5] and platinum,[6,7] and *closo* species with cobalt,[8] nickel,[8,9] and iridium.[10] In addition *closo* bimetallic species containing either two nickel atoms (Ni_2CB_7 framework),[8] or both a nickel and cobalt atom ($CoNiCB_7$)[11] are known.

The *arachno* monocarbaborane anion $[CB_8H_{13}]^-$, shown below, provides a suitable precursor for MCB_8 derivatives *via* reactions with metal halide compounds. The anion itself is well characterised;[12,13] it is isoelectronic with both the borane anion $[B_9H_{14}]^-$ and the dicarbaborane $C_2B_7H_{13}$. All three species possess the same framework structure,

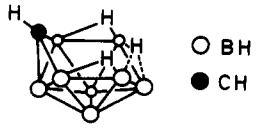

apart from the expected differences in the positioning of the heteroatom(s) and hydrogen atoms about the open face of the cluster. We now report the preparation of two *nido*-MCB_8 (M = Ru or Os) compounds, and also an *arachno*-MCB_8 derivative of ruthenium which shows an interesting comparison with the more common *nido* derivatives.

Results and Discussion

The reaction of the *arachno* anion $[CB_8H_{13}]^-$ with the ruthenium halide derivative [RuCl(CO)(H)$(PPh_3)_3$] in benzene yields the red crystalline complex *nido*-[(CO)$(PPh_3)_2$$RuCB_8H_{10}(PPh_3)$], (**1**), in 54% yield after purification by t.l.c. The corresponding orange osmium compound [(CO)$(PPh_3)_2$Os-$CB_8H_{10}(PPh_3)$], (**2**), was obtained in 34% yield by a similar procedure [equation (1)].

$$Li[CB_8H_{13}] + [MCl(CO)(H)(PPh_3)_3] \longrightarrow [(CO)(PPh_3)_2MCB_8H_{10}(PPh_3)] + 2H_2 + LiCl \quad (1)$$

The n.m.r. spectra of both (**1**) and (**2**) are consistent with the crystal structures, as discussed below, where the metal atom is co-ordinated into the triangular portion of the open face of the *arachno*-carbaborane, to yield the ten-vertex decaborane-like framework. In (**1**) the co-ordination of the $Ru(CO)(PPh_3)_2$ group renders all the cage boron atoms distinct. Although the eight expected resonances are observed in the ^{11}B n.m.r. spectrum, two show coincidental overlap (Table 1). The ^1H n.m.r. spectrum exhibits resonances from seven B–H (terminal) hydrogens, with two B–H–Ru bridging protons lying at higher field, and also a single C–H proton, as well as the protons associated with the aromatic rings of the phosphine ligands. The ^{31}P n.m.r. spectrum shows three resonances from the $Ru(CO)(PPh_3)_2$ fragment, and the cage substituted phosphine.

* 9-Carbonyl-5,9,9-tris(triphenylphosphine)-*nido*-6-carba-9-ruthenadecaborane and -9-osmadecaborane and 9-(η-cyclopentadienyl)-9-hydrido-9-triphenylphosphine-*arachno*-6-carba-9-ruthenadecaborane.

Supplementary data available: see Instructions for Authors, *J. Chem. Soc., Dalton Trans.*, 1987, Issue 1, pp. xvii—xx.

Table 1. Proton and boron-11 n.m.r. data for compounds (1), (2), and (3)

	(1)		(2)			(3)	
Boron assignment *	^{11}B	^{1}H	^{11}B	^{1}H	Boron assignment *	^{11}B	^{1}H
8	23.2	3.98	18.4	4.57	4	20.8	4.1
7	11.1	3.43	11.0	3.35	2	11.0	3.3
1,3	8.2	3.22	6.9	3.77	10	−9.9	2.5
1,3	4.8	2.98	2.8	3.53	5,7	−11.3	2.54
5	−4.8		−6.0		5,7	−11.3	0.9
10	−4.8	2.73	−6.5	3.29	8	−17.2	2.2
2,4	−11.6	1.83	−13.5	2.90	1,3	−29.8	1.2
2,4	−16.8	0.02	−23.7	−0.23	1,3	−31.2	0.7
C(6)–H(*exo*)		6.0		6.1	C(6)–H(*exo*)		1.0
B(8)–H–M(9)		−8.9		−8.9	C(6)–*H*(*endo*)		0.1
B(10)–H–M(9)		−8.72		−8.67	B(5)–H–B(10)		−2.1
					B(7)–H–B(8)		−2.3
					M(9)–H		−9.5
PPh_3		6.9—7.5		6.9—7.7	PPh_3		7.3—7.5
					C_5H_5		4.8

* These assignments have been deduced as described in the text from decoupling experiments. They should be regarded as tentative in view of some of the uncertainties involved.

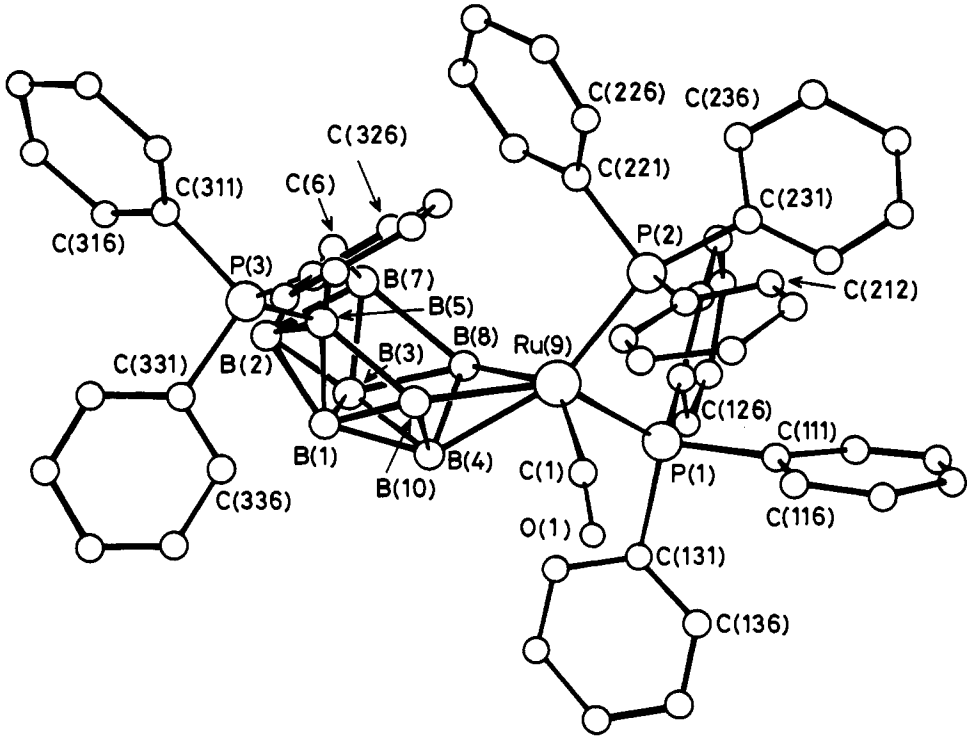

Figure 1. View of (1) showing the atomic numbering (H atoms omitted); the phenyl rings are numbered in sequence C(*mn*1)—C(*mn*6)

The presence of the Ru–CO group is confirmed by an i.r. absorption at 1 965 cm^{-1}.

Some assignments of individual resonances can be made by selective decoupling experiments. Thus in the ^{1}H n.m.r. spectrum a series of ^{1}H-{^{11}B} spectra show each of the seven resonances to be associated with a terminal B–H group. In addition the ^{11}B decoupled spectra demonstrate that the resonance with two-fold intensity in the ^{11}B n.m.r. spectrum is only associated with one B–H proton; therefore this resonance arises from the overlapping of B–H and B–PPh_3 resonances.

The two higher field resonances (at −8.72 and −8.9 p.p.m.) in the ^{1}H n.m.r. spectrum are resolved into a doublet and singlet by decoupling the ^{11}B resonances at −4.8 and 23.2 p.p.m. respectively, confirming that these resonances arise from B–H–Ru protons. Broad-band ^{31}P decoupling further resolves the lower field doublet (−8.72 p.p.m.) into a singlet with $^{2}J(^{31}P\text{–Ru–H}) \sim 50$ Hz. This coupling constant is of the order previously reported for such a *trans* coupling,[14] and thus allows unambiguous assignment of resonances to both the B(8) (23.2 p.p.m.), B(10) (−4.8 p.p.m.), and the separate bridging proton resonances in the ^{11}B and ^{1}H n.m.r. spectra respectively (Table 1).

A further effect of the ^{31}P broad-band decoupling on the ^{1}H n.m.r. spectrum is the removal of a small coupling displayed by the C–H resonance, $^{3}J(^{31}P\text{–B–C–}^{1}H) \sim 12.5$ Hz, suggesting that phosphine substitution occurs at one of the B(2) or B(5,7) boron atoms adjacent to the carbon atom of the assumed 9,6-$RuCB_8$ decaborane-like structure. The comparison of ^{11}B shifts of (1) with those of the carbaborane $[CB_9H_{12}]^-$ [15] and the RuB_9 analogue [14] does not enable a definite assignment of the

Table 2. Selected interatomic distances (pm) and interbond angles (°), with estimated standard deviations in parentheses, for *nido*-[9,9,9-(CO)-$(PPh_3)_2$-9,6-$RuCB_8H_{10}$-5-(PPh_3)] (**1**) and *nido*-[9,9,9-(CO)$(PPh_3)_2$-9,6-$OsCB_8H_{10}$-5-(PPh_3)] (**2**)

(*i*) Distances

	(1)	(2)		(1)	(2)
(*a*) From the metal atom (M = Ru or Os)					
M(9)–P(1)	233.9(5)	234.9(4)	M(9)–B(8)	227(2)	226(2)
M(9)–P(2)	239.8(5)	238.1(4)	M(9)–B(10)	236(2)	234(2)
M(9)–B(4)	227(2)	230(2)	M(9)–C(1)	190(2)	175(2)
(*b*) Boron–boron					
B(1)–B(2)	178(3)	180(3)	B(3)–B(4)	190(3)	182(3)
B(1)–B(3)	179(3)	183(2)	B(3)–B(7)	169(3)	178(2)
B(1)–B(4)	178(3)	182(2)	B(3)–B(8)	175(3)	172(2)
B(1)–B(5)	174(3)	178(2)	B(4)–B(8)	186(3)	182(2)
B(1)–B(10)	170(3)	183(2)	B(4)–B(10)	185(3)	187(2)
B(2)–B(3)	172(3)	182(2)	B(5)–B(10)	185(3)	191(3)
B(2)–B(5)	182(3)	175(2)	B(7)–B(8)	194(3)	207(3)
B(2)–B(7)	186(3)	183(2)			
(*c*) Boron–carbon					
C(6)–B(2)	175(3)	173(2)	C(6)–B(5)	154(3)	152(2)
C(6)–B(7)	157(3)	152(2)			
(*d*) Phosphorus–carbon					
P(1)–C(111)	183(2)	184(1)	P(1)–C(121)	183(2)	187(1)
P(1)–C(131)	187(2)	184(1)	P(2)–C(211)	185(2)	188(1)
P(2)–C(221)	178(2)	187(1)	P(2)–C(231)	188(2)	186(1)
P(3)–C(311)	182(2)	181(1)	P(3)–C(321)	182(2)	182(1)
P(3)–C(331)	180(2)	181(1)			
(*e*) Others					
B(5)–P(3)	192(2)	197(1)	C(1)–O(1)	110(2)	122(2)

(*ii*) Angles

	(1)	(2)		(1)	(2)
(*a*) At the metal atom (M = Ru or Os)					
P(1)–M(9)–P(2)	99.8(2)	99.4(1)	B(4)–M(9)–B(8)	48.4(7)	47.0(6)
P(1)–M(9)–C(1)	89.5(6)	90.0(6)	B(4)–M(9)–B(10)	47.1(7)	47.5(5)
P(2)–M(9)–C(1)	97.3(5)	96.7(6)	B(8)–M(9)–B(10)	78.1(7)	78.8(6)
P(1)–M(9)–B(4)	100.0(5)	100.8(4)	P(2)–M(9)–B(4)	159.3(6)	158.5(5)
P(1)–M(9)–B(8)	86.6(6)	85.7(4)	P(2)–M(9)–B(8)	127.2(6)	128.1(5)
P(1)–M(9)–B(10)	145.2(5)	146.3(4)	P(2)–M(9)–B(10)	114.4(5)	113.8(4)
C(1)–M(9)–B(4)	88.9(7)	90.6(8)	C(1)–M(9)–B(8)	135.4(8)	135.1(7)
C(1)–M(9)–B(10)	80.3(8)	80.7(7)			
(*b*) About open face					
B(5)–C(6)–B(7)	114.6(19)	114.2(13)	C(6)–B(7)–B(8)	118.2(17)	117.8(12)
B(7)–B(8)–M(9)	120.2(11)	118.0(10)	B(8)–M(9)–B(10)	78.1(7)	78.8(6)
M(9)–B(10)–B(5)	122.8(12)	122.3(10)	B(10)–B(5)–C(6)	117.4(16)	117.8(12)
(*c*) Open face to cluster base					
M(9)–B(4)–B(1)	119.5(11)	122.2(10)	C(6)–B(2)–B(1)	98.4(14)	102.4(11)
M(9)–B(4)–B(3)	115.7(11)	116.2(10)	C(6)–B(2)–B(3)	98.3(15)	98.5(12)
B(5)–B(1)–B(10)	65.0(13)	63.8(9)	B(7)–B(3)–B(8)	68.5(13)	72.4(11)
(*d*) Ligand to cluster					
P(3)–B(5)–B(1)	121.8(13)	118.9(10)	P(3)–B(5)–B(2)	118.6(13)	120.5(11)
P(3)–B(5)–C(6)	120.2(16)	120.8(11)	P(3)–B(5)–B(10)	116.2(12)	112.4(10)

substitution position to be made, although the asymmetry of the ^{11}B n.m.r. spectrum does favour B(5,7) substitution, as subsequently confirmed by the *X*-ray structure determination of (**1**). The previously noted B–P resonance is therefore assigned to B(5), although the ^{31}P coupling is unresolved.

Of the remaining five unassigned resonances in the ^{11}B n.m.r. spectrum the resonance at 11.1 p.p.m., is far broader than the rest, indicating that it may be due to the remaining boron atom on the open face of the cluster, B(7). Such correlation of resonance between ^{11}B linewidth and cluster position has been noted elsewhere.[14] The four remaining ^{11}B resonances are therefore attributable to B(1,2,3,4), though their unambiguous

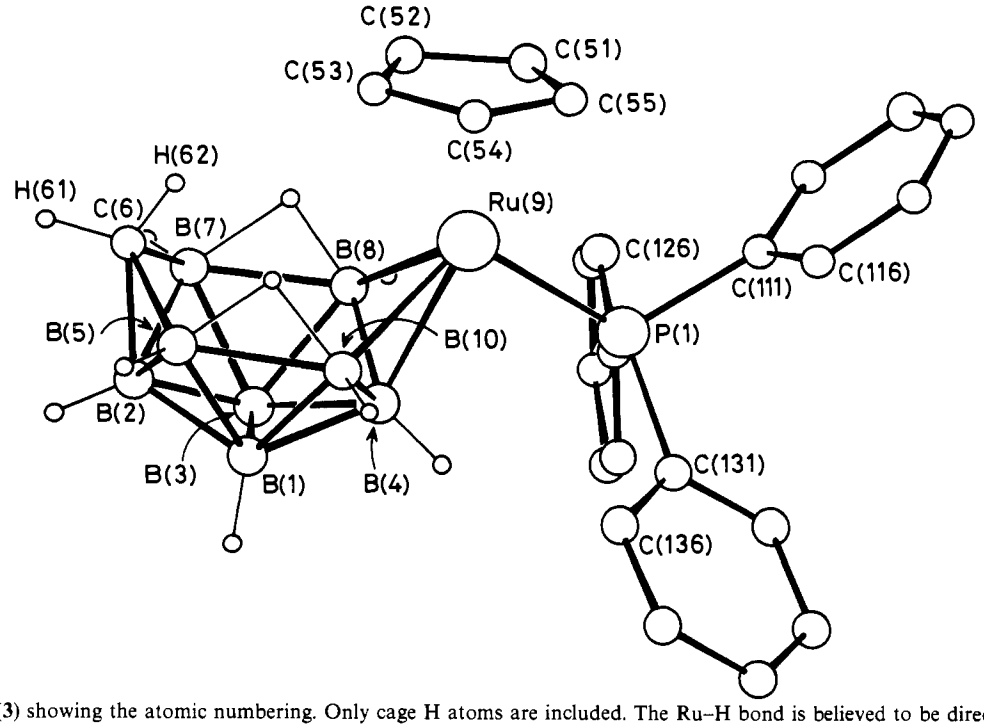

Figure 2. View of (**3**) showing the atomic numbering. Only cage H atoms are included. The Ru–H bond is believed to be directed approximately towards the viewer

assignment is not possible. Tentative assignments have been made by comparison of ^{11}B shielding patterns of (**1**) with those of decaborane(14).[16]

Of the three resonances in the ^{31}P spectrum at 50.1, 39.3, and 8.8 p.p.m., the two low-field resonances both show a small doublet coupling [$^2J(^{31}P–Ru–^{31}P) \sim 25$ Hz], consistent with the *cis* disposition of the phosphine substituents on the ruthenium centre. The resonance at 39.3 p.p.m. also shows the *trans* coupling observed for the lower-field hydride resonance (−8.72 p.p.m.) in the ^1H n.m.r. spectrum, and is therefore assignable to the equatorial phosphine. The high-field resonance, being a broad unresolved quartet, is assigned to the cage bound phosphine.

The ^{11}B, ^1H, and ^{31}P n.m.r. spectra of (**2**) show similarities to those of (**1**) (Table 1). A minor point of interest is that of the three resonances in the ^{31}P n.m.r. spectrum at 18.8, 10.4, and 8.8 p.p.m., the B(cage)–P resonance occurs with exactly the same shift in both (**1**) and (**2**). The other two resonances each show a *cis* coupling [$^2J(^{31}P–Os–^{31}P) \sim 10$ Hz], with the equatorial phosphine having the additional *trans*-coupling [$^2J(^1H–Os–^{31}P) \sim 44$ Hz].

Since we were unable to deduce the position of the cage phosphine substituent relative to the metal *exo*-polyhedral ligands, and because structural parameters were required for comparative purposes with the *arachno* compound described below, *X*-ray diffraction studies of both (**1**) and (**2**) were undertaken.

Compounds (**1**) and (**2**) are isomorphous and show a *nido* ten-vertex cluster, with the carbon and metal atoms in the 6- and 9-positions respectively, and the phosphine cage substituent in the 5-position (Figure 1 shows the ruthenium compound). All skeletal atoms were located, with the presence and position of the bridging and terminal hydrogens being inferred from the n.m.r. data as discussed above. The carbon atom was identified from the observed bond distances and thermal parameter behaviour. Principal bond distances and angles are given in Table 2.

The phosphine substituent is found to be *syn* with respect to the carbonyl ligand on the ruthenium atom, which probably arises from a steric requirement. The metal bound phosphines are mutually *cis*, one being *trans* to a bridging hydrogen. Because the space group is centrosymmetric, both enantiomers of this chiral molecule are present within the unit cell.

All bond lengths are within the ranges found in previous metallacarbaborane structures. The most notable feature is the short bond distance of ~155 pm between the cage carbon and adjacent boron atoms B(5,7) in the open face of the cluster, compared with that of ~175 pm to the boron atom B(2) in the basal plane. This may indicate an sp^2 like bonding mode for the C–H group, directed more towards the open face of the cluster, with the tangential *p* orbital involved in bonding to the basal boron atom [B(2)]. The axial phosphine shows a Ru–P distance some 5 pm longer than that for the *cis* phosphine ligand.

The co-ordination geometry at the ruthenium atom is that of a distorted octahedron, with Ru–P(2) and Ru–B(4) being the axial vectors and with Ru–P(1), Ru–CO, Ru–H(8,9), and Ru–H(9,10) vectors lying in the downward distorted equatorial plane.

The osmium complex (**2**) shows no gross deviations in skeletal geometry or interatomic distance in comparison to (**1**). The same pattern of bonding at the carbon–boron and metal–phosphine vectors is also found. The B(cage)–P(3) distance is marginally shorter in (**1**) than in (**2**), and the carbon of the carbonyl group is some 15 pm closer to the osmium atom than is found in the ruthenium analogue. However, other distances around the osmium atom mirror the pattern found in the ruthenium analogue.

A formal electron count where the metal atom provides two electrons and three orbitals for the skeletal bonding, as Ru^{II}/Os^{II}, gives the twelve electron pairs required for a *nido* structure based on the octadecahedron.[17] The metal atoms thus adopt an 18e configuration with a quasi-octahedral geometry; two of the three bonding orbitals involved in the cluster are largely associated with the two bridging hydrogen atoms between B(8) and B(10) and the metal, with the other being more involved in the metal–B(2) bond. This cluster is an analogue of the recently reported ruthenium(II) borane $[(CO)(PPh_3)_2RuB_9H_{11}(PPh_3)]$;[14] the need for the presence of

Table 3. Selected interatomic distances (pm) and interbond angles (°), with estimated standard deviations in parentheses, for *arachno*-[9,9,9-(η-C_5H_5)(H)(PPh_3)-9,6-$RuCB_8H_{12}$] (**3**)

(*i*) Distances			
(*a*) From the ruthenium atom			
Ru(9)–P(1)	231.1(1)	Ru(9)–C(55)	219.3(5)
Ru(9)–C(51)	222.2(5)	Ru(9)–B(4)	225.2(5)
Ru(9)–C(52)	229.8(5)	Ru(9)–B(8)	231.6(5)
Ru(9)–C(53)	228.5(5)	Ru(9)–B(10)	230.3(6)
Ru(9)–C(54)	222.4(5)		
(*b*) Boron-boron			
B(1)–B(2)	172.0(10)	B(3)–B(4)	176.6(9)
B(1)–B(3)	178.0(10)	B(3)–B(7)	177.4(9)
B(1)–B(4)	178.0(10)	B(3)–B(8)	178.8(9)
B(1)–B(5)	180.7(9)	B(4)–B(8)	176.1(7)
B(1)–B(10)	178.6(9)	B(4)–B(10)	178.2(8)
B(2)–B(3)	172.3(11)	B(5)–B(10)	190.4(10)
B(2)–B(5)	176.9(10)	B(7)–B(8)	186.3(11)
B(2)–B(7)	177.4(10)		
(*c*) Boron–carbon			
C(6)–B(2)	166.0(7)	C(6)–B(5)	171.2(9)
C(6)–B(7)	173.6(10)		
(*d*) Phosphorus–carbon			
P(1)–C(111)	183.6(5)	P(1)–C(121)	183.1(4)
P(1)–C(131)	184.5(4)		
(*ii*) Angles			
(*a*) At the ruthenium atom			
P(1)–Ru(9)–C(51)	96.2(2)	B(4)–Ru(9)–B(8)	45.3(2)
P(1)–Ru(9)–C(52)	127.4(2)	B(4)–Ru(9)–B(10)	46.1(2)
P(1)–Ru(9)–C(53)	155.0(2)	B(8)–Ru(9)–B(10)	78.9(2)
P(1)–Ru(9)–C(54)	127.4(2)	B(4)–Ru(9)–C(51)	149.1(2)
P(1)–Ru(9)–C(55)	95.8(1)	B(4)–Ru(9)–C(52)	126.8(2)
P(1)–Ru(9)–B(4)	79.7(2)	B(4)–Ru(9)–C(53)	124.6(2)
P(1)–Ru(9)–B(8)	89.8(2)	B(4)–Ru(9)–C(54)	143.5(3)
P(1)–Ru(9)–B(10)	111.9(1)	B(4)–Ru(9)–C(55)	172.5(2)
(*b*) About open face			
B(5)–C(6)–B(7)	110.7(4)	C(6)–B(7)–B(8)	115.9(5)
B(7)–B(8)–Ru(9)	122.1(3)	B(8)–Ru(9)–B(10)	78.9(2)
Ru(9)–B(10)–B(5)	121.3(3)	B(10)–B(5)–C(6)	115.6(5)
B(5)–H(510)–B(10)	89.3(29)	B(7)–B(78)–B(8)	87.9(22)
C(6)–B(5)–H(510)	93.0(23)	C(6)–B(7)–H(7,8)	94.7(19)
Ru(9)–B(10)–H(510)	88.2(25)	Ru(9)–B(8)–H(7,8)	87.4(20)
B(2)–C(6)–H(61)	108.7(25)	B(5)–C(6)–H(61)	118.6(29)
B(7)–C(6)–H(61)	117.6(29)	B(2)–C(6)–H(62)	143.3(50)
B(5)–C(6)–H(62)	93.2(41)	B(7)–C(6)–H(62)	105.5(50)
H(61)–C(6)–H(62)	107.2(57)		
(*c*) Open face to cluster base			
Ru(9)–B(4)–B(1)	124.0(3)	C(6)–B(2)–B(1)	111.3(5)
Ru(9)–B(4)–B(3)	125.1(3)	C(6)–B(2)–B(3)	112.9(5)
B(5)–B(1)–B(10)	64.0(4)	B(7)–B(3)–B(8)	63.1(4)

the phosphine on the cage in (**1**) and (**2**) to provide the extra skeletal electron for the *nido* cage is clearly apparent. Further comparisons of (**1**) and (**2**) with the *arachno* compound (**3**) are given below.

The compound *arachno*-[(η-C_5H_5)(H)(PPh_3)$RuCB_8H_{12}$], (**3**), was obtained as yellow crystals in good yield from the action of $[CB_8H_{13}]^-$ on [$RuCl(\eta\text{-}C_5H_5)(PPh_3)_2$] in diethyl ether–benzene. A possible pathway may involve the formation of a cationic ruthenium species [equation (2)], followed by metathesis and loss of a phosphine ligand from the ruthenium centre [equation (3)].

$$[RuCl(\eta\text{-}C_5H_5)(PPh_3)_2] \longrightarrow [Ru(\eta\text{-}C_5H_5)(PPh_3)_2]^+ + Cl^- \quad (2)$$

$$Li[CB_8H_{13}] + [Ru(\eta\text{-}C_5H_5)(PPh_3)_2]Cl \longrightarrow [(\eta\text{-}C_5H_5)(H)(PPh_3)RuCB_8H_{12}] + LiCl + PPh_3 \quad (3)$$

The structure of (**3**) cannot be deduced unambiguously from the ^{11}B n.m.r. data. Though less likely than the favoured 9,6-substituted decaborane(14)-like structure, subsequently confirmed by crystallographic determination, a 10,5- (or even 8,5) subrogated framework as found for the [(η-C_5H_5)$CoC_2B_7H_{11}$] cluster,[18] would, in principle, be expected to yield the observed n.m.r. behaviour.

Whilst the presence of the $RuH(\eta\text{-}C_5H_5)(PPh_3)$ fragment renders the eight cage borons inequivalent, in this case also a coincidental overlap of two resonances occurs and only seven resonances are observed (Table 1). The thirteen cage hydrogens may be detected in the ^1H n.m.r. spectrum, and identified as arising from eight terminal B–H, two bridging B–H–B, two C–H, and one Ru–H. The η-bonded cyclopentadienyl and phosphine ligands are also observed, while the ^{31}P n.m.r. spectrum shows a single resonance as expected at 39.3 p.p.m. The hydride resonance from the Ru–H bond exhibits two couplings, one from the adjacent phosphorus atom of the phosphine ligand, which occupies a position *cis* to the hydride [$^2J(^{31}P\text{–}Ru\text{–}^{31}P) \sim 29$ Hz]. The other smaller coupling [^3J(H–Ru–B–H) ~ 5 Hz] in this 9,6-substituted cluster structure arises from a three-bond coupling to a terminal B–H proton on either the B(8) or B(10) atom bonded to the metal in the open face of the cluster. The coupling is removed by selective decoupling of the three terminal B–H resonances near +2.5 p.p.m., although the off-resonance effect did not allow the unambiguous identification of the precise β-hydrogen involved. In addition decoupling ($^1H\text{–}^1H$) of the lower-field bridging B–H–B atom causes a sharpening of the Ru–H resonance, whereas the same operation with the high-field bridging B–H–B has comparatively little effect. These observations would be compatible with the Ru–H being disposed to one side of the open face of the cluster; while the Ru–H was not detected in the crystal-structure determination, the relative positions of the η-C_5H_5 and PPh_3 ligands around the metal centre confirm this location. The substantial difference between the P(1)–Ru(9)–B(8) and P(1)–Ru(9)–B(10) angles [89.8(2) and 111.9(1)°] indicates that the metal–hydrogen bond is on the same side of the metal as B(10) (*i.e.* towards the viewer in Figure 2). The high-field C–H resonance is also sharpened on decoupling ($^1H\text{–}^1H$) the bridging B–H–B protons, and thus arises from the *endo*-C–H while the low-field C–H resonance is due to the *exo*-C–H proton.

The effects of selective ^{11}B and ^1H decoupling on the ^1H n.m.r. spectrum again allows correlation of the ^{11}B and ^1H spectra, and some limited assignments of the resonances (Table 1). A summary of the important details is as follows. Selective decoupling of the three broader ^{11}B resonances at −9.9(1 B), −11.3(2 B), and −17.2(1 B) p.p.m. sharpens the resonances from the bridging hydrogens at −2.1 and −2.3 p.p.m., thus identifying these four boron atoms as being those in the open face of the cluster B(5,7,8,10). More specifically, decoupling of the ^{11}B resonance at −11.3 p.p.m. sharpens both of the proton resonances (B–H–B) at −2.1 and −2.3 p.p.m., strongly suggesting that this resonance is due to the two boron atoms B(5,7), since of the four in the open face these are the two most likely to possess similar chemical and electronic environments, in the absence of any *endo*-cage substitution. Decoupling the ^{11}B resonance at −9.9 p.p.m. sharpens the bridging hydrogen resonance at −2.1 p.p.m., and since the Ru–H resonance sharpens in the ^1H n.m.r. spectrum on decoupling this low-field bridging hydrogen (−2.1

p.p.m.), identifies the lower-field ^{11}B resonance (−9.9 p.p.m.) as being due to B(10). Of the four remaining boron resonances, those at −29.8 and −31.2 p.p.m. are tentatively assigned to B(1,3) atoms because of their similar environment within the cluster. Decoupling the ^{11}B resonance at 20.8 p.p.m. results in a slight sharpening of the resonance from the Ru–H proton, and this resonance has therefore been assigned to B(4). By elimination the remaining B(2) position has been assigned to the resonance at 11.0 p.p.m.

The structure of (3) determined by a single-crystal *X*-ray diffraction study is shown in Figure 2. The overall geometry of the cluster resembles that of the *arachno*-$[B_{10}H_{14}]^{2-}$ anion, as indicated by the position of the two bridging hydrogens on the open face of the cluster, and the CH_2 group at the apical vertex.

The ruthenium atom achieves eight-co-ordination, with the carbaborane ligand and cyclopentadienyl ligands both occupying three-co-ordination sites. The remaining two-co-ordination sites are occupied by the phosphine and hydride ligands. The increase in co-ordination number of the ruthenium in this compound compared to (1) results from the loading of the metal with the cylopentadienyl ligand in addition to the phosphine, carbaborane, and hydride.

All interatomic distances and angles are in the expected range (Table 3) though differences between the gross geometry of this *arachno* cluster and the *nido* compounds (1) and (2) are found. The presence of a CH_2 group in the open face of the cluster is indicative of the *arachno* class of carbaboranes. The distances from the carbon atom to adjacent boron atoms have a more even distribution than found in the *nido* clusters (1) and (2), with the shortest bond now that to B(2) in the basal plane. The angular disposition of B(2), H(61), and H(62) about the carbon is approximately tetrahedral. This can be interpreted as an sp^3 hybridised carbon with strong bonds to the two attached hydrogens and B(2), with the fourth orbital involved in bonding to the adjacent borons B(5,7) on the open face.

The fundamental difference in cluster geometry, expected from a Wade type of structural classification,[17] between the *nido* compounds (1) and (2) and the *arachno* derivative (3), is their conformity to eleven-and twelve-vertex polyhedra respectively, namely the octadecahedron and icosahedron. Though small, such differences in geometry should manifest themselves in the length and breadth of the open face of the cluster, since in the two cases the open face should be so disposed as to accommodate one and two unoccupied vertices respectively. In the present examples such differences are not marked, because of the overwhelming size of the metal atoms. However, the width of the *arachno* cluster (3) [B(5) to B(7)] is some 25 pm greater than in the *nido* compounds (1) and (2). Such a widening is expected in an *arachno* ten-atom cluster, because it should conform to the icosahedral structure less two vertices, rather than the more condensed eleven-vertex *nido* octadecahedral structure in which one vertex is unoccupied.

Compound (3) presents an interesting problem with regard to the usual electron counting procedure, where for a metallaborane -carbaborane system the metal attains the 18e configuration. The ruthenium centre may be considered as participating in two two-electron three-centre bonds with B(4), B(8), and B(10). However, the structure as a whole may be seen as being similar to either the *arachno*-$[B_{10}H_{14}]^{2-}$ anion, with the CH_2 and metal vertices subrogating the two BH_2^- vertices, or more appropriately the neutral analogue *arachno*-6,9-$C_2B_8H_{14}$, with one of the CH_2 vertices subrogated by the RuH(η-C_5H_5)(PPh_3) fragment. In electron counting terms the electrons in the *endo*-B–H (or C–H) bond of the BH_2 (or CH_2) groups in $[B_{10}H_{14}]^{2-}$ (or $C_2B_8H_{14}$) are included in the skeletal electron count (26e) in order to achieve the number necessary for the *arachno* structures. However, it has been pointed out that the electrons in the *endo*-terminal bond are not necessarily involved in the delocalised cluster orbitals. Therefore in the present structure (3), even though the Ru–H group is not *endo* with respect to the $RuCB_8$ cage, an *arachno* count can still be combined with a Ru^{IV} oxidation state. Two of the 4e contributed by the metal to the skeletal electron count are directly involved in Ru–cage bonding, and two can be arbitrarily taken as those in the Ru–H bond. This problem of achieving both a correct skeletal electron count and a satisfactory metal oxidation state has been encountered before, but not always resolved satisfactorily. In some metallaboranes, such as [4,4,4,4-(CO)(H)(PMe_3)$_2$-4-IrB_8H_{12}], an *arachno* structure is observed although the terminal Ir–H bond does not show any interaction with the cluster.[19] The platinacarbaborane, [(PPh_3)$_2$$PtCB_8$-$H_{12}$], shows similar cage geometry and bond distances to those in (3), but has been classified as a *nido* structure,[20] although from its geometry an *arachno* description is clearly better. These structures can be understood in the same way as (3), as having *arachno* skeletal electron counts achieved by including 2e donated directly from the metal centre to the cluster bonding, and 2e formally donated from the Ir–H bond or from a lone pair on the platinum, which are not involved in the cluster bonding.

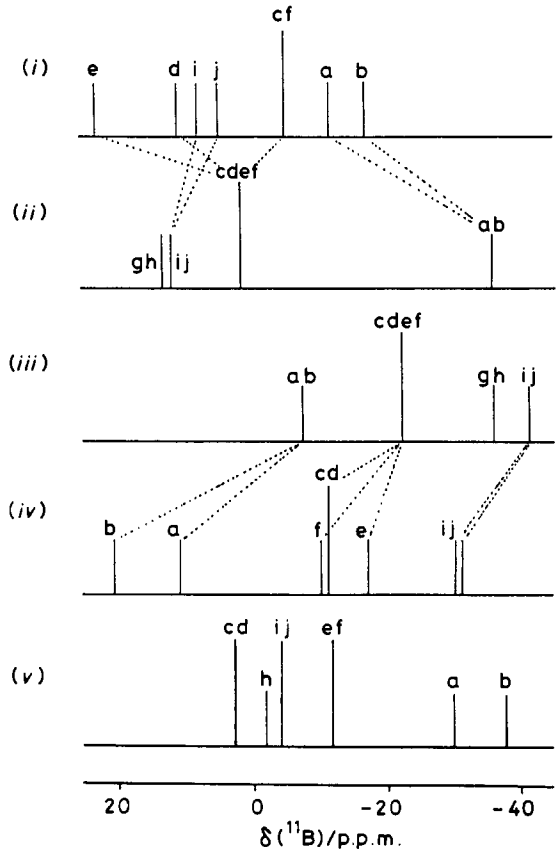

Figure 3. Line diagram of ^{11}B n.m.r. positions in (*i*) *nido*-[(CO)(PPh_3)$_2$-$RuCB_8H_{10}$(PPh_3)] (1), (*ii*) *nido*-$B_{10}H_{14}$, (*iii*) *arachno*-$[B_{10}H_{14}]^{2-}$, (*iv*) *arachno*-[(η-C_5H_5)(H)(PPh_3)$RuCB_8H_{12}$] (3), and (*v*) *nido*-$[CB_9H_{12}]^-$. Assignments for the cage framework atoms are a, B(2); b, B(4); c, B(5); d, B(7); e, B(8); f, B(10); g, B(6); h, B(9); i, B(1); and j, B(3). Resonances are assigned as from Table 1, and the $[CB_9H_{12}]^-$ from ref. 15

Finally, in the light of the above discussion a further interesting comparison can be made between the ^{11}B n.m.r. spectra of compounds (1) and (3) and those of the isoelectronic boron hydrides $B_{10}H_{14}$ and $[B_{10}H_{14}]^{2-}$ respectively (Figure 3). The most immediate observation of the trends within these four sets of spectra is the reversal of the B(1,3) and B(2,4) shifts between

Table 4. Crystal data, collection and refinement parameters

Compound	(1)	(2)	(3)
Formula	$C_{56}H_{55}B_8P_3Ru$	$C_{56}H_{55}B_8OsP_3$	$C_{24}H_{33}B_8PRu$
System	Monoclinic	Monoclinic	Monoclinic
Space group	$P2_1/n$	$P2_1/n$	$P2_1/n$
Absences	← $h0l$; $h + l = 2n + 1$ and $0k0$; $k = 2n + 1$ →		
a/Å	17.023(7)	17.009(6)	12.642(2)
b/Å	13.628(7)	13.634(4)	14.832(5)
c/Å	22.353(7)	22.469(9)	14.327(4)
β/°	103.38(3)	103.65(3)	108.46(2)
U/Å^3	5 045(4)	5 087(3)	2 548(1)
M	1 024.5	1 113.6	540.0
D_c/g cm^{-3}	1.35	1.45	1.41
D_m/g cm^{-3}	1.33	1.50	1.48
Z	4	4	4
μ(Mo-K_α)/cm^{-1}	4.37	26.41	6.77
F(000)	2 112	2 240	1 104
Total reflections	6 733	6 891	4 806
Reflections with $I/\sigma(I) \geqslant 3.0$	2 670	3 525	3 523
$2\theta_{max.}$/°	50	50	50
Range (2θ) about $K_{\alpha1-\alpha2}$/position/°	+/−1.0	+/−1.0	+/−1.1
Transmission factors (max.–min.)	—	0.73—0.57	0.92 − 0.88
Crystal size/mm	—	0.52 × 0.24 × 0.47	0.7 × 0.3 × 0.55
g	0.0070	0.0014	0.000 53
R	0.087	0.050	0.046
R'	0.089	0.050	0.047
Max./min. on final ΔF map/e Å^{-3}	1.2, −0.7	1.5, −1.0	0.9, −1.1
Final max. shift/error	0.27	0.5	0.03

Table 5. Final fractional co-ordinates (× 10^4), with estimated standard deviations in parentheses, for *nido*-[9,9,9-(CO)(PPh_3)$_2$-9,6-$RuCB_8H_{10}$-5-(PPh_3)] (1)

Atom	x	y	z	Atom	x	y	z
Ru(9)	3 275.7(10)	6 435.6(10)	6 091.1(6)	C(212)	3 893(15)	4 123(15)	7 730(9)
B(1)	4 053(13)	8 704(15)	5 764(9)	C(213)	4 003(19)	4 146(19)	8 378(11)
B(2)	4 651(13)	8 547(16)	5 215(8)	C(214)	4 224(23)	5 045(19)	8 680(10)
B(3)	3 656(14)	8 179(14)	5 020(9)	C(215)	4 464(20)	5 878(17)	8 343(10)
B(4)	3 169(13)	7 977(13)	5 695(8)	C(216)	4 316(14)	5 770(12)	7 730(8)
B(5)	4 968(13)	8 093(14)	5 998(9)	C(221)	4 908(14)	4 939(11)	6 488(9)
C(6)	5 087(14)	7 418(12)	5 471(8)	C(222)	5 159(12)	5 220(12)	5 964(9)
B(7)	4 319(15)	7 296(16)	4 933(10)	C(223)	5 896(12)	5 137(14)	5 834(10)
B(8)	3 297(14)	7 005(14)	5 140(9)	C(224)	6 534(19)	4 722(14)	6 329(11)
B(10)	4 085(14)	7 855(15)	6 327(9)	C(225)	6 268(12)	4 398(13)	6 873(8)
P(1)	1 982(3)	5 841(3)	5 650(2)	C(226)	5 575(12)	4 524(14)	6 928(9)
P(2)	3 891(3)	4 964(3)	6 571(2)	C(231)	3 551(11)	3 681(13)	6 341(7)
P(3)	5 886(3)	8 693(3)	6 540(2)	C(232)	2 933(14)	3 264(13)	6 497(8)
C(1)	2 890(12)	6 916(13)	6 769(8)	C(233)	2 748(14)	2 311(13)	6 316(10)
O(1)	2 671(9)	7 284(10)	7 137(6)	C(234)	3 113(12)	1 789(14)	6 024(8)
C(111)	1 538(13)	4 996(13)	6 115(8)	C(235)	3 768(17)	2 180(18)	5 829(9)
C(112)	995(11)	4 216(15)	5 865(9)	C(236)	3 990(15)	3 153(14)	6 001(8)
C(113)	725(12)	3 621(15)	6 238(9)	C(311)	6 796(11)	8 762(11)	6 249(7)
C(114)	857(11)	3 706(14)	6 831(9)	C(312)	7 524(15)	8 450(15)	6 592(9)
C(115)	1 338(12)	4 471(13)	7 115(8)	C(313)	8 233(15)	8 609(19)	6 370(11)
C(116)	1 655(15)	5 106(14)	6 750(8)	C(314)	8 219(13)	9 133(15)	5 813(10)
C(121)	1 876(11)	5 147(11)	4 935(7)	C(315)	7 450(18)	9 412(16)	5 505(11)
C(122)	2 344(12)	4 409(13)	4 894(8)	C(316)	6 771(13)	9 241(13)	5 722(9)
C(123)	2 297(15)	3 808(14)	4 375(9)	C(321)	6 193(13)	8 020(13)	7 261(7)
C(124)	1 641(15)	3 986(14)	3 880(10)	C(322)	6 535(14)	8 517(15)	7 821(8)
C(125)	1 090(15)	4 738(16)	3 921(9)	C(323)	6 772(15)	7 963(17)	8 349(10)
C(126)	1 181(14)	5 309(13)	4 428(8)	C(324)	6 696(14)	6 993(16)	8 382(11)
C(131)	1 165(11)	6 784(12)	5 462(7)	C(325)	6 378(18)	6 527(15)	7 811(11)
C(132)	1 281(12)	7 536(11)	5 066(8)	C(326)	6 095(19)	7 023(16)	7 280(10)
C(133)	690(12)	8 216(16)	4 907(8)	C(331)	5 693(12)	9 927(13)	6 780(8)
C(134)	−13(17)	8 187(15)	5 096(10)	C(332)	6 175(16)	10 699(14)	6 669(10)
C(135)	−108(14)	7 432(15)	5 473(10)	C(333)	6 009(17)	11 655(19)	6 862(11)
C(136)	504(12)	6 745(13)	5 658(8)	C(334)	5 393(14)	11 788(12)	7 169(9)
C(211)	4 018(13)	4 940(12)	7 416(8)	C(335)	4 997(15)	11 053(17)	7 240(9)
				C(336)	5 125(14)	10 090(14)	7 038(9)

Table 6. Final fractional co-ordinates ($\times 10^4$), with estimated standard deviations in parentheses, for *nido*-[9,9,9-(CO)$(PPh_3)_2$-9,6-$OsCB_8H_{10}$-5-(PPh_3)] (**2**)

Atom	*x*	*y*	*z*	Atom	*x*	*y*	*z*
Os(9)	3 272.9(3)	6 453.5(4)	6 089.8(3)	C(212)	5 156(9)	5 250(10)	5 952(7)
B(1)	4 051(10)	8 796(12)	5 749(8)	C(213)	5 922(9)	5 118(12)	5 864(8)
B(2)	4 667(10)	8 546(14)	5 217(7)	C(214)	6 496(11)	4 702(12)	6 311(8)
B(3)	3 614(10)	8 181(13)	5 025(7)	C(215)	6 334(10)	4 402(12)	6 852(10)
B(4)	3 179(11)	8 007(12)	5 681(8)	C(216)	5 575(9)	4 505(11)	6 953(7)
B(5)	4 961(9)	8 115(12)	5 967(8)	C(221)	3 565(9)	3 719(10)	6 317(7)
C(6)	5 087(9)	7 425(10)	5 467(6)	C(222)	3 992(10)	3 192(10)	5 974(7)
B(7)	4 354(10)	7 312(12)	4 936(7)	C(223)	3 756(10)	2 245(11)	5 811(7)
B(8)	3 261(10)	7 035(12)	5 146(8)	C(224)	3 141(11)	1 825(11)	5 988(7)
B(10)	4 083(9)	7 852(13)	6 330(7)	C(225)	2 703(11)	2 322(12)	6 316(8)
P(1)	1 983(2)	5 839(3)	5 644(2)	C(226)	2 926(8)	3 301(11)	6 475(7)
P(2)	3 888(2)	4 994(3)	6 563(2)	C(231)	4 029(9)	4 963(11)	7 411(6)
P(3)	5 889(2)	8 704(3)	6 550(2)	C(232)	3 891(11)	4 108(12)	7 731(7)
C(1)	2 925(10)	6 881(13)	6 717(9)	C(233)	4 024(15)	4 161(16)	8 363(8)
O(1)	2 695(7)	7 267(9)	7 134(5)	C(234)	4 260(15)	5 034(14)	8 674(8)
C(111)	1 533(7)	4 987(10)	6 107(5)	C(235)	4 412(13)	5 843(14)	8 360(8)
C(112)	1 045(8)	4 219(10)	5 846(6)	C(236)	4 289(11)	5 796(11)	7 724(7)
C(113)	726(9)	3 584(12)	6 197(6)	C(311)	6 782(8)	8 782(9)	6 247(6)
C(114)	856(9)	3 698(11)	6 802(7)	C(312)	6 757(9)	9 253(11)	5 700(7)
C(115)	1 335(9)	4 491(12)	7 074(7)	C(313)	7 434(9)	9 403(13)	5 483(7)
C(116)	1 683(9)	5 131(12)	6 724(7)	C(314)	8 185(11)	9 130(13)	5 857(7)
C(121)	1 179(8)	6 791(10)	5 440(6)	C(315)	8 242(9)	8 635(13)	6 376(7)
C(122)	494(9)	6 758(10)	5 657(7)	C(316)	7 540(9)	8 437(11)	6 583(7)
C(123)	−108(10)	7 456(12)	5 490(8)	C(321)	5 728(9)	9 960(10)	6 768(6)
C(124)	−28(10)	8 182(11)	5 103(7)	C(322)	5 110(10)	10 113(12)	7 047(7)
C(125)	662(10)	8 243(11)	4 886(7)	C(323)	4 977(10)	11 073(12)	7 247(8)
C(126)	1 262(9)	7 544(11)	5 053(6)	C(324)	5 442(11)	11 807(11)	7 162(7)
C(131)	1 833(8)	5 156(10)	4 918(6)	C(325)	6 046(14)	11 646(12)	6 863(9)
C(132)	2 388(9)	4 430(11)	4 886(6)	C(326)	6 172(10)	10 761(11)	6 677(8)
C(133)	2 253(10)	3 856(12)	4 355(7)	C(331)	6 196(8)	8 050(11)	7 266(6)
C(134)	1 595(9)	4 018(11)	3 865(6)	C(332)	6 139(11)	7 038(12)	7 274(7)
C(135)	1 095(8)	4 732(11)	3 922(6)	C(333)	6 418(11)	6 522(13)	7 822(7)
C(136)	1 199(8)	5 303(10)	4 431(6)	C(334)	6 712(9)	6 990(13)	8 352(7)
C(211)	4 954(8)	4 926(10)	6 476(7)	C(335)	6 770(11)	7 975(14)	8 359(8)
				C(336)	6 509(9)	8 502(12)	7 815(6)

Table 7. Final fractional co-ordinates ($\times 10^4$), with estimated deviations in parentheses, for *arachno*-[9,9,9-(η-C_5H_5)(H)(PPh_3) -9,6-$RuCB_8H_{12}$] (**3**)

Atom	*x*	*y*	*z*	Atom	*x*	*y*	*z*
Ru(9)	2 225.6(3)	7 212.1(2)	7 709.1(2)	C(122)	2 745(4)	8 664(3)	10 660(4)
B(1)	5 178(5)	7 461(5)	8 387(4)	C(123)	2 805(4)	9 541(4)	11 019(4)
B(2)	5 262(5)	8 288(5)	7 572(4)	C(124)	2 136(6)	10 198(4)	10 482(4)
B(3)	4 683(5)	8 572(4)	8 471(4)	C(125)	1 385(5)	9 998(3)	9 565(4)
B(4)	3 928(5)	7 635(4)	8 683(4)	C(126)	1 336(4)	9 138(3)	9 199(4)
B(5)	4 834(6)	7 201(5)	7 093(4)	C(131)	2 678(4)	6 578(3)	10 220(3)
C(6)	4 318(5)	8 173(4)	6 469(4)	C(132)	2 445(4)	6 597(3)	11 106(3)
B(7)	4 043(6)	8 966(4)	7 253(5)	C(133)	2 988(4)	6 003(3)	11 857(3)
B(8)	3 192(5)	8 563(4)	8 021(4)	C(134)	3 740(4)	5 386(3)	11 737(3)
B(10)	4 012(5)	6 730(4)	7 891(4)	C(135)	3 958(4)	5 355(3)	10 846(4)
P(1)	1 901.0(9)	7 324.6(7)	9 203.9(8)	C(136)	3 448(4)	5 949(3)	10 107(3)
C(51)	513(4)	7 591(4)	6 786(4)	H(01)	5 919(46)	7 255(33)	8 886(41)
C(52)	1 210(5)	7 857(4)	6 241(4)	H(02)	5 993(41)	8 536(31)	7 536(34)
C(53)	1 723(5)	7 076(4)	6 037(3)	H(03)	5 112(44)	9 007(37)	9 065(40)
C(54)	1 340(5)	6 338(4)	6 441(4)	H(04)	4 008(38)	7 517(30)	9 412(33)
C(55)	584(4)	6 657(4)	6 900(3)	H(05)	5 363(44)	6 720(37)	6 812(38)
C(111)	481(4)	6 968(3)	9 112(3)	H(61)	4 640(39)	8 390(32)	5 969(34)
C(112)	−421(4)	7 544(4)	9 001(4)	H(62)	3 609(63)	7 903(48)	6 125(58)
C(113)	−1 474(4)	7 221(4)	8 844(4)	H(07)	4 051(42)	9 653(32)	7 118(37)
C(114)	−1 677(4)	6 318(4)	8 811(4)	H(08)	2 831(35)	9 102(29)	8 341(29)
C(115)	−801(4)	5 727(3)	8 945(4)	H(10)	4 199(36)	6 001(30)	8 058(31)
C(116)	257(4)	6 047(3)	9 100(3)	H(78)	2 933(34)	8 664(29)	7 107(31)
C(121)	2 009(4)	8 449(3)	9 754(3)	H(510)	3 789(45)	6 836(39)	6 922(40)

the *nido* and *arachno* clusters, and moreover the general agreement in pattern between the borane and heteroborane examples within each structural classification. Clearly, this agreement is more easily seen in compound (**3**), where there is no *endo*-cage substitution adding to the asymmetry of the cluster. The high-field shift of the B(2,4) and B(1,3) resonances in the *nido* and *arachno* compounds is further evidence of the observation[21] that a boron atom which connects two other

boron atoms bridged by a hydrogen atom on the open face will have a high-field shift. In the case of (**1**) and (**2**), whilst no bridging hydrogen is present to indicate such an effect at B(2), the distribution of the electron density within the cage is presumably similar to the MB_9 cage analogues, *e.g.* $[(PMe_2Ph)_3OsB_9H_{13}]$, where there are indeed such bridge bonds, and B(2) also moves to lower field although to a slightly lesser extent than in the present examples.[2] A comparison with the ^{11}B n.m.r. spectrum of the $[CB_9H_{12}]^-$ ion, which is isoelectronic with $B_{10}H_{14}$, can also be made, but the general conclusions remain the same. The absence of any theory which allows a predicted shift of resonances between isoelectronic species, especially those which are charged and uncharged, limits the discussion. However, it is worthwhile noting that, as has been pointed out for metallaborane clusters,[2] it does appear that even the presence of a further heteroatom (carbon) in the framework does not perturb the electronic distribution to such an extent that the relative positions of the B(1,3) and B(2,4) resonances are changed. Finally, a notable downfield shift is observed for B(8) in the *nido* compounds (**1**) and (**2**) where there is a phosphine substituent in the antipodal B(5) position.

Experimental

All reactions were carried out under a dry, oxygen-free nitrogen atmosphere using conventional Schlenk apparatus. The carbaborane CB_8H_{14} was prepared as described elsewhere.[12] The compounds $[RuCl(CO)(H)(PPh_3)_3]$, $[OsCl(CO)(H)(PPh_3)_3]$, and $[RuCl(\eta\text{-}C_5H_5)(PPh_3)_2]$ were prepared by standard methods.[22] Preparative thin layer chromatography was carried out in air using Merck Kieselgel 60 PF_{254} on 20 × 20 × 0.1 cm plates. Solvents were dried by distillation from sodium or $LiAlH_4$, and stored over molecular sieves.

The ^{11}B, ^1H, and ^{31}P n.m.r. spectra were recorded as CD_2Cl_2 solutions on a Bruker WH400 n.m.r. spectrophotometer at 128.0, 400.1, and 162.0 MHz respectively. The $^1H\text{-}\{^{11}B\}$ spectra were recorded at 360 MHz on a similar spectrophotometer. Infrared spectra were recorded from KBr discs using a Perkin-Elmer 580B spectrophotometer.

Preparation of $[(CO)(PPh_3)_2RuCB_8H_{10}(PPh_3)]$, (**1**).—Butyl-lithium (0.5 cm^3 of a 1.5 mol dm^{-3} diethyl ether solution, 0.75 mmol) was added to a stirred solution of CB_8H_{14} (0.085 g, 0.75 mmol) in benzene (40 cm^3) under nitrogen. After 15 min $[RuCl(CO)(H)(PPh_3)_3]$ (0.7 g, 0.73 mmol) was added and the solution refluxed for 30 min. The solvent was removed under vacuum from the resulting orange-red solution. Chromatography of the orange solid using CH_2Cl_2–light petroleum (1:1, b.p. 60—80 °C) yielded the product (**1**) (R_f = 0.2).

Recrystallisation from CH_2Cl_2–light petroleum gave 0.41 g (0.4 mmol, 54%) of the product. Red polygonal plate-like crystals, suitable for *X*-ray diffraction analysis, were grown by slow diffusion of light petroleum into a CH_2Cl_2 solution.

Preparation of $[(CO)(PPh_3)_2OsCB_8H_{10}(PPh_3)]$, (**2**).—The compound was prepared in an essentially identical procedure to that described for the ruthenium analogue. From CB_8H_{14} (0.05 g, 0.44 mmol), reaction and subsequent chromatography in benzene, yielded 0.17 g (0.15 mmol, 34%) of the orange compound (R_f = 0.3). Crystals were grown by the diffusion method described above.

Preparation of $[(\eta\text{-}C_5H_5)(H)(PPh_3)RuCB_8H_{12}]$, (**3**).—Butyl-lithium (0.7 cm^3 of a 1.3 mol dm^{-3} diethyl ether solution, 0.91 mmol) was added to a stirred solution of CB_8H_{14} (0.1 g, 0.89 mmol) in benzene (30 cm^3) and diethyl ether (20 cm^3) under nitrogen. After 15 min $[RuCl(\eta\text{-}C_5H_5)(PPh_3)_2]$ (0.64 g, 0.88 mmol) was added and the mixture refluxed for 48 h. A yellow turbid solution was produced, which gave a yellow precipitate on cooling. After removal of the solvent under vacuum, the solid was extracted with CH_2Cl_2 and recrystallised from CH_2Cl_2–light petroleum to yield 0.32 g (0.59 mmol, 67%) of product.

Slow evaporation of a CH_2Cl_2 solution gave yellow diamond block crystals, which were used for the *X*-ray structure determination.

Analyses on all the above compounds gave poor results, especially for the carbon and metal content. The compounds have therefore been characterised from their n.m.r. spectra and the structural studies.

Crystal Structure Analysis.—The crystal data, collection and structure refinement parameters for (**1**), (**2**), and (**3**) are given in Table 4 (λ = 0.710 69 Å, T = 290 K). Data were collected with a Syntex $P2_1$ four-circle diffractometer operating in the θ–2θ mode, with scan speeds in the range 2–29° min^{-1}, depending on the intensity of a 2-s pre-scan; backgrounds were measured at each end of the scan for 0.25 of the scan time. Three standard reflections were monitored every 200 reflections, and any slight changes were corrected by rescaling. Unit-cell dimensions and standard deviations were obtained by least-squares fit to 15 high-angle reflections. Only observed reflections $[I/\sigma(I) \geqslant 3.0]$ were used in refinement, corrected for Lorentz, polarisation and absorption effects, the last with ABSCOR[23] for (**3**) and by the Guassian method for (**2**). Data for compound (**1**) were not absorption corrected due to loss of the crystal before its dimensions were established, but in view of the modest effect on the other compounds this should not be serious. The poor R value for (**1**) is attributed to its weak diffracting power; virtually no diffraction was observed above 40° and the ratio of observed to unobserved reflections is only 0.4. For each compound, the heavy atom was located by the Patterson technique and the light atoms then found on successive Fourier syntheses. Hydrogen atoms were given fixed isotropic thermal parameters, U = 0.007 $Å^2$, with those defined by the molecular geometry being inserted at calculated positions and not refined. Cage H atoms could not be located for (**1**) and (**2**), but were located and refined with isotropic thermal parameters for (**3**). The metal hydrogen in (**3**) could not be found. Final refinement was on F by cascaded least-squares methods with anisotropic thermal parameters for all atoms other than hydrogen. Weighting schemes of the form $w = 1/[\sigma^2(F) + gF^2]$ were used, and shown to be satisfactory by a weight analysis. Computing was with the SHELXTL system[24] on a Data General DG30. Scattering factors in the analytical form and anomalous dispersion factors were taken from ref. 25. Final atomic coordinates are given in Tables 5—7.

Acknowledgements

We thank the S.E.R.C. for a grant in support of this work, Johnson Matthey plc for the loan of ruthenium and osmium salts, and Drs. I. H. Sadler and D. Reed, University of Edinburgh, for recording the ^{11}B and ^{31}P decoupled ^1H n.m.r. spectra.

References

1 J. D. Kennedy, *Prog. Inorg. Chem.*, 1986, **34**, 211.
2 M. A. Beckett, N. N. Greenwood, J. D. Kennedy, and M. Thornton-Pett, *J. Chem. Soc., Dalton Trans.*, 1986, 795 and refs. therein.
3 N. N. Greenwood, M. J. Hails, J. D. Kennedy, and W. S. McDonald, *J. Chem. Soc., Dalton Trans.*, 1985, 953.
4 J. R. Bowser, A. Bonny, J. R. Pipal, and R. N. Grimes, *J. Am. Chem. Soc.*, 1979, **101**, 6229.
5 J. E. Crooks, N. N. Greenwood, J. D. Kennedy, and W. S. McDonald, *J. Chem. Soc., Chem. Commun.*, 1981, 933.

6 K. Base, B. Stibr, and I. Zakharova, *Synth. React. Inorg. Metal-Org. Chem.*, 1980, **10**, 509.
7 K. Base, B. Stibr, G. A. Kukina, and I. A. Zakharova, Proc. 8th Conf. Coord. Chem., Slovak Chem. Soc., Bratislava, Czechoslovakia, December, 1980, pp. 17—19.
8 B. Stibr, Z. Janousek, K. Base, J. Dolansky, S. Hermanek, K. A. Solntsev, L. A. Butman, I. I. Kuznetsov, and N. T. Kuznetsov, *Polyhedron*, 1982, **1**, 833; *Collect. Czech. Chem. Commun.*, 1984, **49**, 1660.
9 C. G. Salentine, R. R. Rietz, and M. F. Hawthorne, *Inorg. Chem.*, 1974, **13**, 3025.
10 N. W. Alcock, J. G. Taylor, and M. G. H. Wallbridge, *J. Chem. Soc., Chem. Commun.*, 1983, 1168.
11 C. G. Salentine and M. F. Hawthorne, *J. Am. Chem. Soc.*, 1975, **97**, 6382.
12 K. Base, B. Stibr, J. Dolansky, and J. Duben, *Collect. Czech. Chem. Commun.*, 1981, **46**, 2345.
13 O. W. Howarth, M. J. Jasztal, and M. G. H. Wallbridge, *Polyhedron*, 1985, **4**, 1461.
14 N. N. Greenwood, J. D. Kennedy, M. Thornton-Pett, and J. D. Woollins, *J. Chem. Soc., Dalton Trans.*, 1985, 2397.
15 O. W. Howarth, M. J. Jasztal, and M. G. H. Wallbridge, unpublished work.
16 G. R. Eaton and W. N. Lipscomb, 'N.M.R. Studies of Boron Hydrides and Related Compounds,' W. A. Benjamin Inc., New York, 1969.
17 K. Wade, *Adv. Inorg. Chem. Radiochem.*, 1976, **18**, 1.
18 K. P. Calahan, F. Y. Lo, C. E. Strouse, A. L. Sims, and M. F. Hawthorne, *Inorg. Chem.*, 1974, **13**, 2842.
19 J. Bould, J. E. Crook, N. N. Greenwood, and J. D. Kennedy, *J. Chem. Soc., Dalton Trans.*, 1984, 1903.
20 G. A. Kukina, M. A. Porai-Koshits, V. S. Sergienko, Yu. V. Zefirov, and G. G. Sadikov, *Koord. Khim.*, 1985, **11**, 385 (*Chem. Abstr.*, 1985, **103**, 123679).
21 S. Hermanek and J. Plesek, *Z. Anorg. Allg. Chem.*, 1974, **409**, 115.
22 M. I. Bruce, C. Hameister, A. G. Swincer, and T. C. Wallis, *Inorg. Synth.*, 1982, **21**, 78.
23 N. W. Alcock, in 'Crystallographic Computing,' ed. F. Ahmed, Munksgaard, Copenhagen, 1970.
24 G. M. Sheldrick, SHELXTL User Manual, Nicolet Instrument Co., Wisconsin, 1981.
25 'International Tables for *X*-Ray Crystallography,' Kynoch Press, Birmingham, 1974, vol. 4.

Received 15*th January* 1987; *Paper* 7/074